Polymer Chemistry

Ring-Opening Metathesis Polymerization-Induced Self-Assembly (ROMPISA) of a Cisplatin Analogue for High Drug-Loaded Nanoparticles

Journal:	*Polymer Chemistry*
Manuscript ID	PY-COM-10-2018-001539.R2
Article Type:	Communication
Date Submitted by the Author:	23-Mar-2019
Complete List of Authors:	Wright, Daniel; Northwestern University, Chemistry Proetto, Maria; Northwestern University, Chemistry Touve, Mollie; Northwestern University, Chemistry Gianneschi, Nathan; Northwestern University, Chemistry; University of California, San Diego, Chemistry and Biochemistry

Polymer Chemistry

COMMUNICATION

Ring-Opening Metathesis Polymerization-Induced Self-Assembly (ROMPISA) of a Cisplatin Analogue for High Drug-Loaded Nanoparticles

Received 00th January 20xx,
Accepted 00th January 20xx

DOI: 10.1039/x0xx00000x

www.rsc.org/

Daniel B. Wright,[a]† Maria T. Proetto,[a]† Mollie A. Touve[a] and Nathan C. Gianneschi*[a]

We report the one-pot aqueous phase synthesis of cisplatin drug loaded micellar nanoparticles using Ring-Opening Metathesis Polymerization-Induced Self-Assembly (ROMPISA). ROMPISA was used to generate a small library of nanoparticles to examine the effect of size and charge on their action as cytotoxic agents against human ovarian and cervical cancer cells *in vitro*. The results show that polymerization-induced self-assembly (PISA) can easily yield drug loaded nanoparticles in one step at high solids concentrations in water for formulation of drugs at cytotoxic levels.

Commonly, platinum-based drug polymer nanomedicines are routinely formulated via non-covalent encapsulation of the drug into the core of a specifically designed nanoparticle carrier.[1-4] These platinum-based nanoparticles have shown notable advantages over the conventional small molecule platinum analogues.[3-6] However, these polymer particles are typically difficult to formulate at high drug loadings per particles and in addition, at high solids concentrations in the final formulation of the overall material.[1, 2] Although polymers with covalently bound platinum-based drugs can overcome limitations of drug loading capacity per particle, they are generally subject to formulation at low solids concentrations in solution. Moreover, the majority of polymerization approaches lack the ability to directly polymerize platinum containing monomers and rely instead on post-polymerization modification.[7, 8]

Polymerization-induced self-assembly (PISA) is capable of. effectively and rapidly producing morphologies with a desired range of sizes in solution.[9-23] Moreover, the PISA methodology can be performed at high solids concentrations, up to 50 wt%.[11] Although predominantly limited to radical based methods, PISA has recently been expanded to Ring-Opening Metathesis Polymerization (ROMP), coined Ring-Opening Metathesis Polymerization-Induced Self-Assembly (ROMPISA).[24, 25] In addition, ROMPISA is amenable to the aqueous phase, giving nanostructures in a controlled manner and in one step.[25] One of the attractive features of choosing ROMP as the polymerization strategy for a PISA process is the strong tolerance of certain initiators to a diverse range of functionalities, which renders it useful for the direct polymerization of functional monomers.[26-33]

In this paper, our approach was to employ ROMPISA in water using a quaternary amine Hoveyda-Grubbs 2nd generation initiator for direct, one-pot incorporation of a platinum-based drug into nanoparticles (Scheme 1). Specifically, we planned to incorporate poly(oligo ethylene glycol) stabilizer blocks and then directly chain extend with a cisplatin analogue norbornene dicarboximide derivative, to form spherical micelles with varying sizes and platinum loadings at much higher solids concentrations than previously explored by conventional methods. In addition, a pH responsive cisplatin particle was prepared to explore charge and pH effects on interactions with cellular membrane and endosomes during in vitro delivery and uptake.[7]

To begin, an oligo ethylene glycol (OEG) macro-stabilizer block was synthesized *in situ* to a degree of polymerization (DP) of 20 utilizing a quaternary amine Hoveyda-Grubbs 2nd generation initiator (Scheme 1a). An aliquot was removed for ^{1}H NMR spectroscopy (NMR) and size exclusion chromatography (SEC) for further analysis. Subsequently a mixture of cisplatin analogue norbornene dicarboximide (Scheme 1b), and quaternary amine phenyl norbornene dicarboximide were added, in a molar ratio of 1:3, to a final concentration of 5 w/w%, where the targeted copolymer DPs were 20, 25 and 50 (respectively **20-20**, **20-25** and **20-50**, Table 1). A mixture of two monomers were used to improve the core block solubility upon

[a] *Department of Chemistry, Department of Materials Science and Engineering, and Department of Biomedical Engineering, Northwestern University, 2145 Sheridan Road, Evanston, Illinois 60208-3113, United States of America. E-mail: nathan.gianneschi@northwestern.edu*

† D.B.W. and M.T.P. contributed equally to this work. Electronic Supplementary Information (ESI) available: [Synthesis of the polymers, additional characterization of polymers and particles via TEM and DLS.]. See DOI: 10.1039/x0xx00000x

the initial formation of nanoparticles in solution. Additionally, a diblock copolymer where a pure cisplatin analogue norbornene dicarboximide block was synthesized with a DP of 20, **20-20$_{Pt}$**.

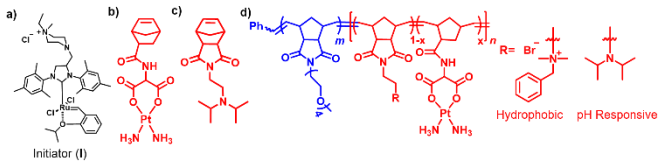

Scheme 1. a) Structure of the aqueous Initiator, (**I**). b) Structure of the cisplatin analogue norbornene dicarboximide. c) Structure of the pH responsive, 2-(diisopropylamino)ethyl norbornene dicarboximide. d) Structure of the amphiphilic diblock copolymer formed. Blue highlights hydrophilic, $N_{OEG,}$ red highlights hydrophobic, N_{Core}.

After 1 h, samples were quenched with ethyl vinyl ether and polymers analyzed by SEC-MALS and NMR, with particles characterized by dynamic light scattering (DLS) and transmission electron microscopy (TEM) (Table 1).

First, NMR analysis showed the consumption of both the cisplatin analogue norbornene dicarboximide and quaternary amine phenyl norbornene dicarboximide together which highlights the formation of a statistical core block, where the cisplatin is distributed throughout the core. Moreover, for each chain extension >99% monomer conversion was observed via NMR. Additionally, SEC-MALS analysis highlighted the low dispersity of the diblock polymers formed and the single monomodal chromatography. A combination of both SEC and NMR deduced the cisplatin analogue norbornene dicarboximide can be successfully polymerized directly in pure water from the OEG macro-stabilizer block (see Figure S1).

Upon polymerization, the quaternary amine phenyl norbornene dicarboximide and cisplatin analogue norbornene dicarboximide are insoluble in water, regardless of core monomer composition, forming a hydrophobic block.[25] TEM and DLS were used to interrogate the formation of the resulting amphiphile self-assemblies. The targeted block lengths of the polymer systems were hypothesized to give spherical micelles in all cases, given the large OEG block which creates a high surface curvature favoring spherical nanostructures. DLS and TEM analysis conclude the formation of spherical micelles *in situ* (Figure 1, see Figure S2). Although the morphology of the particles does not change with block length, what can be observed is that the size of the particles increase as the block length increases.

In addition to the P(OEG)-b-P(cisplatin analogue norbornene dicarboximide-co-quaternary amine phenyl norbornene

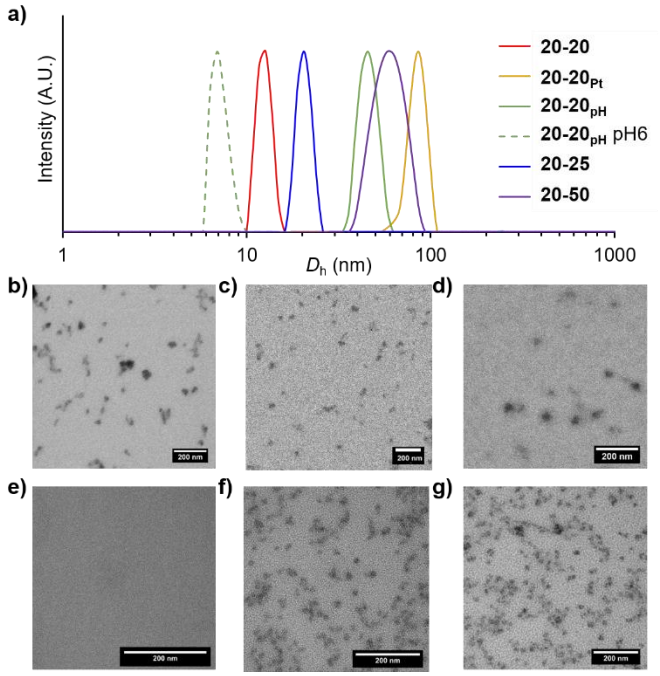

Figure 1. a) Distribution of hydrodynamic radius from DLS for the particles formed by the cisplatin functionalized block copolymers. TEM micrographs for the particles formed by b) **20-20**. c) **20-20$_{Pt}$** d) **20-20$_{pH}$** e) **20-20$_{pH}$** at pH 6 f) **20-25**g) **20-50**. Scale bar 200 nm.

dicarboximide) diblock copolymers, a second pH-responsive block copolymer was synthesized via ROMPISA, **20-20$_{pH}$**. Here a 2-(diisopropylamino)ethyl norbornene dicarboximide monomer is used to form the copolymer block with the cisplatin analogue norbornene dicarboximide (Scheme 1). Where at basic and neutral conditions the amine is deprotonated and is hydrophobic while in acidic conditions the amine is hydrophilic.[7] From a combination of both SEC and NMR it could be observed that this responsive monomer did not influence the ROMPISA methodology and polymerization yielded low dispersity dispersity material (Table 1). The resulting ROMPISA nanoparticles were analyzed via DLS and TEM and, in addition, the pH-responsive behavior was investigated. Both DLS and TEM confirmed the presence of spherical nanoparticles in solution at neutral pH yet when the pH of the solution is lowered to pH 6 the particles disassemble as expected.

Table 1. Molecular characterization of the cisplatin functionalized block copolymers.

Polymer[a]	$M_{n\ Theo}$[b] (kDa)	$M_{n\ SEC}$[c] (kDa)	$Đ$[c]	N_{OEG} (m)[c]	N_{core} (n)[c]	X[d]	*Wt% Pt*	D_h (nm)[e]	Zeta Potential (mV)
20-20	15.5	17.7	1.10	20	20	0.33	17	13	5.9
20-20$_{Pt}$	16.3	18.1	1.18	20	20	1	54	86	1.2
20-20$_{pH}$[f]	14.0	15.4	1.11	20	20	0.33	20	46	-5.2
20-25	17.2	19.5	1.21	20	25	0.33	20	21	3.9
20-50	28.4	31.5	1.20	20	50	0.33	27	81	2.0

[a] The block length of the blocks for P(OEG)-b-P(cisplatin analogue norbornene dicarboximide-co-quaternary amine phenyl norbornene dicarboximide) and P(OEG)-b-P(cisplatin analogue norbornene dicarboximide-co-2-(diisopropylamino)ethyl norbornene dicarboximide). [b]Determined by monomer conversion from 1H NMR spectroscopy. [c]Calculated from SEC-MALS in DMF. [d]Mol % of cisplatin analogue norbornene dicarboximide in the second block 2-(diisopropylamino)ethyl norbornene dicarboximide). e Determined by DLS. [f] Denotes the comonomer is 2-(diisopropylamino)ethyl norbornene dicarboximide).

Polymer Chemistry

COMMUNICATION

(Figure 1). Interestingly, zeta potential measurements showed that the incorporation of the 2-(diisopropylamino)ethyl norbornene dicarboximide) monomer in the core influenced the charge in the nanoparticle surface from an overall positive to negative charge. A similar effect on surface charge is observed for **20-20**, **20-25** and **20-50**, where an increase of dicarboximide-*co*-quaternary amine phenyl norbornene monomer in the core, decreased the overall charge (Table 1).

Additionally, scanning transmission electron microscopy Energy-dispersive X-ray spectroscopy (STEM-EDX) was used to analyze the platinum loading in the spherical micelles (Figure 2, example is **20-50**). Initially, from brightfield STEM a large contrast signal is observed for the ROMPISA particles which indicates high-Z atoms are present. STEM-EDX analysis shows the presence of platinum in the ROMPISA particles. Therefore, STEM-EDX results deduce the incorporation of cisplatin into the micelles.

Next, *in vitro* cytotoxicity to human cervical cancer (HeLa) and ovarian cancer (CAOV3) cell lines was examined. The set of nanoparticles (Table 1) together with cisplatin alone, were tested for 96 h against both cells lines at a concentration of 80, 40 and 20 μM with respect to platinum. It is important to highlight, that all nanoparticle suspensions were formulated keeping vehicle concentrations (in our case water) below 1%, even for the 80 μM ones. This is highly desirable when designing cytotoxicity studies to avoid vehicle interference with cellular function and it was enabled by our ROMPISA strategy which yielded stock nanoparticle suspension at high solids concentrations (Pt concentration > 100 mM) in water in one step. All the nanoparticles showed concentration dependent cytotoxic effects against both cell lines (Figure 3).

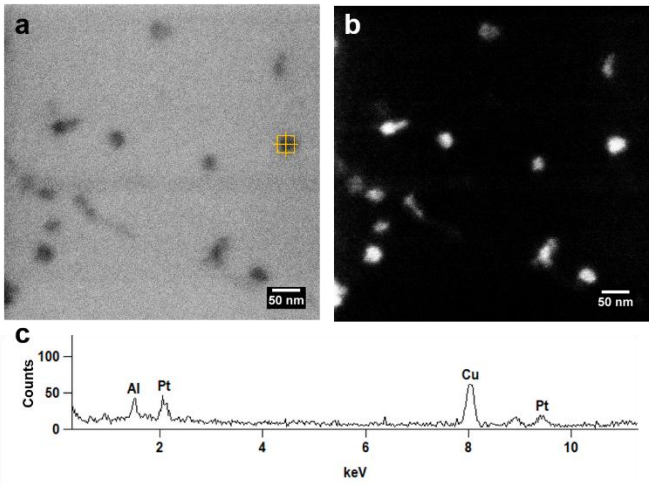

Figure 2. STEM-EDX characterization for **20-50**. a) Brightfield STEM and b) HAADF STEM micrographs of unstained particles. c) EDX Spectrum taken from the area boxed in 2a. Insert scale bar 50 nm.

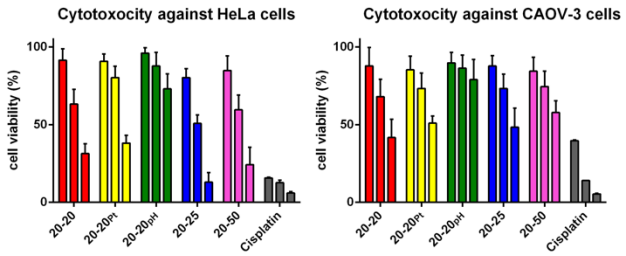

Figure 3. Cytotoxic activity of nanoparticles **20-20**, **20-20$_{Pt}$**, **20-20$_{pH}$**, **20-25** and **20-50** against HeLa (left) and CAOV3 (right) cells determined by the CellTiter-Blue assay after 96 h of incubation and expressed % cell viability compared to cells treated with the nanoparticle's vehicle (water). A nanoparticle suspension containing either 20, 40 or 80 μM (left to right columns for each formulation) with respect to platinum was used for the assay and it is shown as increasing concentrations from left to right for each nanoparticle set. HeLa and CAOV3 cell lines were sourced from American Type Culture Collection (ATCC).

Cellular associated platinum was analyzed via Inductively Coupled Plasma Mass Spectrometry (ICP-MS) as an indirect measurement of nanoparticle uptake (Figure 4). As expected, the largest amount of platinum was obtained from HeLa cells exposed to **20-20** and **20-25**, which at the same time show the highest cytotoxic activity and smaller diameter (13 nm and 21 nm respectively). In general, lower uptake was observed in CAOV3 cells, and this agrees with the lower cytotoxicity observed. **20-20$_{pH}$** showed the lowest uptake on both cells lines, as well as the least cytotoxicity. Moreover, at 80 μM, all nanoparticles showed at least 50% inhibition of cellular growth except **20-20$_{pH}$** and **20-50** against CAOV3 cells. Interestingly, the most active micelles were **20-25** (against HeLa cells) and **20-20** (against CAOV3 cells), unexpectedly even more active than **20-20$_{pt}$**, which has the highest drug loading per particle.

It is well known that nanoparticle size and surface charge or zeta potential, among other factors, have a strong influence on their cellular uptake and ability to deliver different amounts of drug intracellularly.[34-36] For this set of nanoparticles, smaller sizes were observed to have enhanced uptake and increased cytotoxicity. Additionally, nanoparticle surface charge appears to have a crucial influence on uptake and as a consequence cytotoxicity. It is well described that nonphagocytic cells uptake positively charged nanoparticles better than their uncharged or negatively charged counterparts.[37] In our studies, this was also observed for uptake of the nanoparticles by HeLa cells, where positively charged nanoparticles where taken up to higher degrees than the negatively charged **20-20$_{pH}$** and among the positively charged ones, the uptake increased with the increase in surface charge (**20-20**>**20-25**>**20-50**>**20-20$_{Pt}$**). This is likely because of the stronger affinity of positively charged nanoparticles for the negatively charged cell membrane.[34]

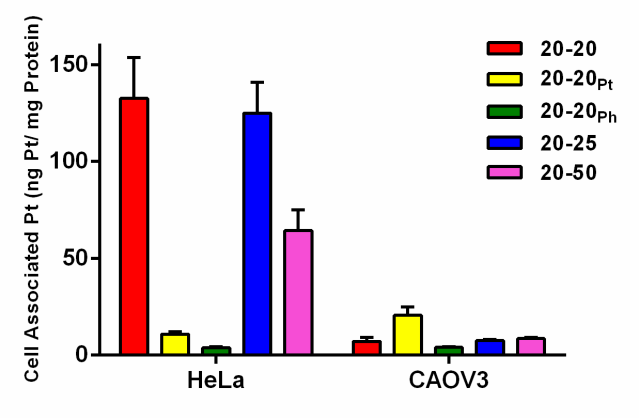

Figure 4. Platinum associated to HeLa (left) and CAOV3 (right) cells preincubated with **20-20**, **20-20**$_{Pt}$, **20-20**$_{pH}$, **20-25** and **20-50** at a 5 μM platinum concentration for 6 h and analyzed by ICP-MS.

Conclusions

In conclusion, the ROMPISA protocol has been extended for a range of platinum loaded particles for potential application as antitumor agents. We could demonstrate NP activity is related to nanoparticle uptake which is influenced by nanoparticle size and zeta potential. Together, these data lead us to strive for a more complete understanding of drug release and how it correlates with in vitro cytotoxicity in time. Polymer architecture and surface charge of the particle create a complex interplay of factors that are not easily replicated in cell free assays. Indeed, in related studies, we have shown that no platinum drug release is observed in cell free assays, and yet cytotoxicity and in vivo activity can be observed, including drug release in cells and tissues, as evidenced by multimodal imaging.[38] Ongoing efforts in our laboratory focus on these questions of polymer architecture and particle surface charge optimization with respect to release kinetics in terms of tuning for sustained versus burst release in a more predictable fashion. Finally, PISA provides a route to high weight percent particle in solution in a single pot,[15] a fact exploited in a range of applications including viscosity modifiers, cell encapsulation.[15] We exploit the PISA methodology here, demonstrating an initial example of the direct incorporation of a drug into a particle core. With PISA capable of achieving high concentrations of drug-loaded nanoparticles we envision rapidly formulating materials for low volume injections at high dose in small animal models of human disease.

Acknowledgements

This research was conducted with support from DoD through a MURI from the Air Force Office of Scientific Research (FA-9550-16-1-0150) and a National Defense Science and Engineering Graduate (NDSEG) Fellowship, 32 CFR 168a, to M.A.T. This work made use of the BioCryo facility of Northwestern University's NUANCE Center, which has received support from the Soft and Hybrid Nanotechnology Experimental (SHyNE) Resource (NSF ECCS-1542205); the MRSEC program (NSF DMR-1720139) at the Materials Research Center; the International Institute for Nanotechnology (IIN); and the State of Illinois, through the IIN. Dr. Swagat Sahu is kindly thanked for the quaternary amine phenyl norbornene dicarboximide. Ms. Ziying Hu is thanked for zeta potential measurements. Apeiron Catalysts, Inc., are thanked for the generous donation of the aqueous initiator (Aquamet).

Conflicts of interest

There are no conflicts to declare

Notes and references

1. C. Pinto Reis, R. J. Neufeld, A. J. Ribeiro and F. Veiga, *Nanomedicine*, 2006, **2**, 8-21.
2. T. Doane and C. Burda, *Adv. Drug Deliv. Rev.*, 2013, **65**, 607-621.
3. V. T. Huynh, J. Y. Quek, P. L. de Souza and M. H. Stenzel, *Biomacromolecules*, 2012, **13**, 1010-1023.
4. N. Nishiyama, S. Okazaki, H. Cabral, M. Miyamoto, Y. Kato, Y. Sugiyama, K. Nishio, Y. Matsumura and K. Kataoka, *Cancer Res.*, 2003, **63**, 8977-8983.
5. A. S. Paraskar, S. Soni, K. T. Chin, P. Chaudhuri, K. W. Muto, J. Berkowitz, M. W. Handlogten, N. J. Alves, B. Bilgicer, D. M. Dinulescu, R. A. Mashelkar and S. Sengupta, *Proc. Natl. Acad. Sci.,* 2010, **107**, 12435-12440.
6. S. Dhar, N. Kolishetti, S. J. Lippard and O. C. Farokhzad, *Proc. Natl. Acad. Sci.*, 2011, **108**, 1850-1855.
7. M. T. Proetto, C. R. Anderton, D. Hu, C. J. Szymanski, Z. Zhu, J. P. Patterson, J. K. Kammeyer, L. G. Nilewski, A. M. Rush, N. C. Bell, J. E. Evans, G. Orr, S. B. Howell and N. C. Gianneschi, *ACS Nano*, 2016, **10**, 4046-4054.
8. R. C. Hayward and D. J. Pochan, *Macromolecules*, 2010, **43**, 3577-3584.
9. J. Tan, H. Sun, M. Yu, B. S. Sumerlin and L. Zhang, *ACS Macro Lett.*, 2015, **4**, 1249-1253.
10. J. Tan, X. Zhang, D. Liu, Y. Bai, C. Huang, X. Li and L. Zhang, *Macromol. Rapid Commun.*, 2016, **38**, 1600508.
11. J. Yeow and C. Boyer, *Adv. Sci.*, 2017, **4**, 1700137.
12. E. R. Jones, M. Semsarilar, P. Wyman, M. Boerakker and S. P. Armes, *Polym. Chem.*, 2016, **7**, 851-859.
13. J. Tan, D. Liu, Y. Bai, C. Huang, X. Li, J. He, Q. Xu, X. Zhang and L. Zhang, *Polym. Chem.*, 2017, **8**, 1315-1327.
14. A. Blanazs, A. J. Ryan and S. P. Armes, *Macromolecules*, 2012, **45**, 5099-5107.
15. S. L. Canning, G. N. Smith and S. P. Armes, *Macromolecules*, 2016, **49**, 1985-2001.
16. L. A. Fielding, M. J. Derry, V. Ladmiral, J. Rosselgong, A. M. Rodrigues, L. P. D. Ratcliffe, S. Sugihara and S. P. Armes, *Chem. Sci.*, 2013, **4**, 2081-2087.
17. L. P. D. Ratcliffe, B. E. McKenzie, G. M. D. Le Bouëdec, C. N. Williams, S. L. Brown and S. P. Armes, *Macromolecules*, 2015, **48**, 8594-8607.

18. N. J. Warren, O. O. Mykhaylyk, D. Mahmood, A. J. Ryan and S. P. Armes, *J. Am. Chem. Soc.*, 2014, **136**, 1023-1033.
19. N. J. Warren, O. O. Mykhaylyk, A. J. Ryan, M. Williams, T. Doussineau, P. Dugourd, R. Antoine, G. Portale and S. P. Armes, *J. Am. Chem. Soc.*, 2015, **137**, 1929-1937.
20. M. Williams, N. J. W. Penfold, J. R. Lovett, N. J. Warren, C. W. I. Douglas, N. Doroshenko, P. Verstraete, J. Smets and S. P. Armes, *Polym. Chem.*, 2016, **7**, 3864-3873.
21. C. A. Figg, R. N. Carmean, K. C. Bentz, S. Mukherjee, D. A. Savin and B. S. Sumerlin, *Macromolecules*, 2017, **50**, 935-943.
22. C. A. Figg, A. Simula, K. A. Gebre, B. S. Tucker, D. M. Haddleton and B. S. Sumerlin, *Chem. Sci.*, 2015, **6**, 1230-1236.
23. S. Jain and F. S. Bates, *Science*, 2003, **300**, 460-464.
24. D. B. Wright, M. A. Touve, L. Adamiak and N. C. Gianneschi, *ACS Macro Lett.*, 2017, **6**, 925-929.
25. D. B. Wright, M. A. Touve, M. P. Thompson and N. C. Gianneschi, *ACS Macro Lett.*, 2018, **7**, 401-405.
26. J. K. Kammeyer, A. P. Blum, L. Adamiak, M. E. Hahn and N. C. Gianneschi, *Polym. Chem.*, 2013, **4**, 3929-3933.
27. M. P. Thompson, L. M. Randolph, C. R. James, A. N. Davalos, M. E. Hahn and N. C. Gianneschi, *Polym. Chem.*, 2014, **5**, 1954-1964.
28. B. Autenrieth and R. R. Schrock, *Macromolecules*, 2015, **48**, 2493-2503.
29. K. Nomura and R. R. Schrock, *Macromolecules*, 1996, **29**, 540-545.
30. R. Singh, C. Czekelius and R. R. Schrock, *Macromolecules*, 2006, **39**, 1316-1317.
31. R. B. Grubbs and R. H. Grubbs, *Macromolecules*, 2017, **50**, 6979-6997.
32. S. H. Hong and R. H. Grubbs, *J. Am. Chem. Soc.*, 2006, **128**, 3508-3509.
33. D. M. Lynn, B. Mohr and R. H. Grubbs, *J. Am. Chem. Soc.*, 1998, **120**, 1627-1628.
34. C. He, Y. Hu, L. Yin, C. Tang and C. Yin, *Biomaterials*, 2010, **31**, 3657-3666.
35. F. Alexis, E. Pridgen, L. K. Molnar and O. C. Farokhzad, *Mol. Pharm.*, 2008, **5**, 505-515.
36. H. Gao, W. Shi and L. B. Freund, *Proc. Natl. Acad. Sci.*, 2005, **102**, 9469-9474.
37. E. Frohlich, *Int. J. Nanomed.*, 2012, **7**, 5577-5591.
38. M. T. Proetto, C. E. Callmann, J. Cliff, C. J. Szymanski, D. Hu, S. B. Howell, J. E. Evans, G. Orr, N. C. Gianneschi, *ACS Cent. Sci.,* 2018, **4,** 1477-1484.